Indian Geotechnical Journal, 31 (2), 2001

Generalised Procedure of Slices for Analysis of Zoned Dams Under Steady Seepage

G. Bhattacharya* and P.K. Basudhar†

Introduction

Determination of critical slope failure surfaces based on limit equilibrium methods valid for general slip surfaces coupled with the Sequential Unconstrained Minimization Technique (SUMT) or the Penalty Function method has now received lot of attention (Greco, 1988; Bhattacharya, 1990). The authors have developed a new procedure called Direct Procedure using Spencer's method (Spencer, 1973) in conjunction with the Extended Interior Penalty Function method (Kavlie, 1971). One of the most distinguishing features of the developed procedure is that it has built-in provisions to ensure that the obtained solutions satisfy some prescribed acceptability criteria. The basic formulation of the technique together with its application in case of homogeneous slopes has been presented elsewhere (Bhattacharya and Basudhar, 2000b). The purpose of this paper is to examine the effectiveness and efficiency of the Direct Procedure when applied to the general case of nonhomogeneous slopes, and, specifically to slopes of zoned dams and embankments.

Analysis of zoned dams and embankments under steady seepage have been reported by several investigators, using various techniques. Baker (1979) reported about the analysis of the Okete Dam upstream slope under steady seepage condition with the help of the program SSOPT which is based on the Spencer method of analysis (Spencer, 1967) in conjunction with the dynamic programming technique. The principle of the methodology adopted in the program SSOPT and its formulation were presented elsewhere (Baker,

* Assistant Professor, Department of Civil Engineering, Bengal Engineering College (A Deemed University), Howrah – 711103, WB, India. E-mail: gautam@civil.becs.ac.in

† Professor, Department of Civil Engineering, Indian Institute of Technology, Kanpur, Kanpur – 208016, India. E-mail: pkbd@iitk.ac.in

1980). Celestino and Duncan (1981) used a simplified search scheme proposed by them to find the critical shear surface for the Birch Dam in Oklahoma, based on the Spencer (1967) method to compute the factor of safety. Later, Nguyen (1985) used the Simplex refection technique in combination with the simplified Bishop method to search for the critical slip surface for the same dam section.

Satyam Babu (1986) analysed the downstream slope of the Beas Dam in Punjab, India, which is founded on a thin shear zone. He used the Interior Penalty Function Method coupled with Janbu's Generalized Procedure of Slices (Janbu, 1973). He also highlighted some numerical difficulties arising due to the presence of the thin shear zone in the foundation. One major deficiency of this approach is that an Interior Penalty Function Method requires a feasible starting point, which may not be readily available. Later, Basudhar et al. (1988) employed a more generalized version of the above approach based on the Sequential Unconstrained Minimization Technique coupled with the Janbu's GPS procedure.

It may be mentioned here that although, in a broad sense, nonhomogeneous slopes also include slopes in soils with anisotropic undrained strength variation, studies on such slopes have been presented elsewhere (Bhattacharya and Basudhar, 2000a) and, therefore, have not been included here. The present paper deals first with the extension to the basic formulation (presented earlier with reference to homogeneous slopes) and then with an illustration of the same to the analysis of slopes of zoned dams and embankments.

Analysis

Discretization Model, Design Variables, Objective Function and Constraints

Figure 1 shows a typical section of a zoned dam along with a potential slip surface of arbitrary shape which terminates at the bottom of a vertical tension crack of depth z_t. Three subsoil layers have been shown in the Figure. There can be, however, any number of layers with any arbitrary alignment. The potential sliding mass is divided into n number of vertical slices. With reference to the chosen system of axes, y and z represent the ordinates of the points on the sheer surface and on the slope boundary respectively corresponding to a particular x-coordinate at an interslice boundary. The shape and location of the slip surface is completely defined by these x- and y-coordinates and the factor of safety can be expressed as a function of these design variables. For finding the critical slip surface, these coordinates, which minimize the factor of safety, need to be determined. The factor of safety is the objective function here.

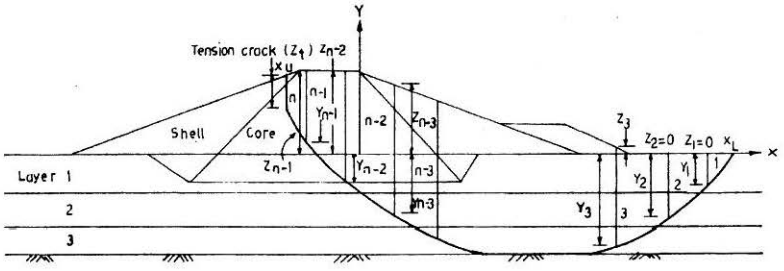

FIGURE 1 : A Typical Section of a Zoned Dam along with a Trial Non-Circular Shear Surface

For the determination of the critical slip surface the Direct Procedure (Bhattacharya and Basudhar, 2000b) valid for methods of analysis satisfying all equilibrium conditions such as the Spencer method (Spencer, 1973) is adopted. In this procedure the problem is formulated as follows.

Find the shape and location of the critical slip surface, together with the associated minimum factor of safety ($F = F_{min}$), subject to the following requirements.

(i) The equilibrium conditions, as expressed by the following equations, are satisfied:

$$\text{Force Equilibrium: } Z_n(F, \theta) = 0 \tag{1a}$$

$$\text{Moment Equilibrium: } M_n(F, \theta) = 0 \tag{1b}$$

In the above, Z_n and M_n are the external balancing force and moment respectively; F is the average factor of safety and θ is a characteristic angle defining the interslice force inclination.

For the expressions for Z_n and M_n, reference may be made to the original work of Spencer (1973) or, for a loaded slope, to Bhattacharya and Basudhar (1992).

(ii) The shape of the critical slip surface as well as the line of thrust obtained as part of the solution are both reasonable.

Design Vector

The design variables are collected in a design vector as follows:

$$\mathbf{D} = [y_2, y_3, \ldots, y_i, \ldots y_n, x_L, x_U, F, \theta]^T \tag{2}$$

where, referring to Fig.1, y_2, y_3, ..., y_n denote the y-coordinates defining the slip surface, while x_L and x_U are the x-coordinates of the lower and the upper points of intersection between the slip surface and the slope boundary.

Design Constraints

Equality Constraint: The requirements in Eqn. (1) are combined to form a single normalised equality constraint as:

$$l_j(\mathbf{D}) = \frac{Z_n^2 + S_f M_n^2}{(\gamma b H_t)^2} \tag{3}$$

where, γ is any characteristic unit weight of soil, b is the width of each slice, H_t is any characteristic height of the slope and S_f is a scale factor introduced to make the function well behaved (Bhattacharya and Basudhar, 1999).

Inequality Constraints : The following inequality constraints are imposed in the analysis to obtain a reasonable critical slip surface and the associated line of thrust.

1. The shear surface must lie within the slope geometry.

$$g_j(\mathbf{D}) = \frac{y_i}{z} - 1 \leq 0 \tag{4}$$

$$i, j = 1, 2, \ldots, n-1$$

2. The shear surface should not penetrate any rigid stratum below. An alternative approach is to impose unusually high values of strength parameters for the rigid layer.

3. The slip surface should have a shape, which is concave upward.

4. To avoid development of tension, the line of thrust, obtained as a part of the solution, must lie within the sliding mass.

5. To avoid unnecessary search an appropriate lower bound on the design variable F may be imposed.

Mathematical forms together with discussions for the constraints 2 through 5 are the same as in homogeneous slopes and are given elsewhere (Bhattacharya and Basudhar, 2000a; 2000b).

Mathematical Programming Formulation and Solution Procedure

The constrained minimization problem stated above can be cast as a mathematical programming problem of the following general form :

Find **D** such that

$$f(\mathbf{D}) \rightarrow \text{Min.} \tag{5a}$$

subject to the constraints : $g_j(\mathbf{D}) \leq 0 \qquad j = 1, 2, \ldots, n_i.$ (5b)

$$l_j(\mathbf{D}) = 0 \qquad j = 1, 2, \ldots, n_e. \tag{5c}$$

where, n_i and n_e are the total number of inequality and equality constraints respectively. **D**, $f(\mathbf{D})$, $g(\mathbf{D})$ and $l(\mathbf{D})$ represent the design vector, the objective function, the inequality and the equality constraint functions respectively.

As an initial feasible decision vector is generally not available, a method, which accepts infeasible starting design vector, is advantageous. The extended penalty function method enunciated by Kavlie (1971) has been used in the present study because of the fact that this method readily accepts infeasible decision points but the optimal solution lies in the feasible region. In this method, the constrained problem is transformed into an unconstrained one as follows:

$$\psi(\mathbf{D}, r_k) = f(\mathbf{D}) - r_k \sum_{j=1}^{p} G_j\left[g_j(\mathbf{D})\right] \tag{6}$$

where, the function G is chosen as follows:

$$\begin{aligned} G\left[g_j(\mathbf{D})\right] &= \frac{1}{g_j(\mathbf{D})} && \text{for } g_j(\mathbf{D}) \leq \varepsilon \\ &= \frac{\left[2\varepsilon - g_j(\mathbf{D})\right]}{\varepsilon^2} && \text{for } g_j(\mathbf{D}) > \varepsilon \end{aligned} \tag{7}$$

where, the tolerance, ε, is given by:

$$\varepsilon = -\frac{r_k}{\delta_t} \tag{8}$$

δ_t is a parameter defining the transition between the two types of penalty terms and p is the total number of constraints. General guidelines for appropriate choice of the parameters δ_t and, ε are available in the literature (Kavlie and Moe, 1971; Cassis and Schmit 1976). r is a positive constant called penalty parameter and r_k is its value corresponding to the k^{th} cycle of minimization. Using a reduction factor c (usual value is 0.10) the penalty parameter r_k is made successively smaller in order to obtain the constrained minimum value of the objective function $f(\mathbf{D})$. Thus,

$$r_{k+1} = c\, r_k \tag{9}$$

The composite function $\psi(\mathbf{D})$ so generated, is then minimized by using Powell's method of conjugate directions for multidimensional search and quadratic interpolation technique for unidimensional search (Fox, 1971).

A Generalised Procedure for Calculation of Slice Characteristics in a Zoned Dam

In the computation of the factor of safety of a heterogeneous dam or embankment section using the method of slices, complications arise in the calculation of weight, mobilised shear force and pore water pressure for each slice. This is because of the fact that the base of a particular slice is most likely to lie in more than one zone or region and below a number of layers or zone boundaries starting from the slope boundary. It is, therefore, required to locate the two end points of the base of a slice so that appropriate values for the soil and pore pressure properties can be used in the calculation of the above mentioned slice characteristics. A generalised procedure for the computation of the weight, the cohesive and frictional components of the shear strength and the resultant pore water pressure for each slice has been developed. It consists of the following steps:

Location of a Slice

This involves the following steps:

1. To draw the slope section to a convenient scale.

2. To introduce a co-ordinate system with the following conventions:

   (i) The horizontal x-coordinate increases in the direction of slide.

   (ii) The vertical y-coordinate increases in the direction of gravity.

   (iii) The origin is conveniently chosen at the mid-point of the top width of the embankment or the dam section so that the y-coordinates of all points in the search region are positive.

3. The trial or given shear surface is drawn and the sliding mass is divided into the selected number of slices which need not be of uniform widths. Thus, the coordinates of the points on the shear surface at its intersections with the interslice boundaries are known. The slope of the base of the kth slice can be calculated from:

$$\tan\alpha_k = \frac{(y_{k+1} - y_k)}{\Delta x_k} \tag{10}$$

where, α_k is the angle made by the base of the k^{th} slice with the horizontal; Δx_k is the width of the kth slice; y_k and y_{k+1} are the ordinates of the points of intersection between the shear surface and the kth and the $(k+1)^{th}$ slice boundaries respectively i.e., the ordinates of the two ends of the base of the kth slice.

4. To introduce a vertical boundary at every point where the slope surface and the boundary between layers change directions. Such points are herein called the 'intersection points' of the slope section. When either the slope surface or any of the layer boundaries has a vertical section, two vertical boundaries are introduced at the same x i.e., a strip of zero thickness is assumed in between. Thus the entire search region is divided into a number of parts along the horizontal x-direction. Each of these parts is herein termed as a 'range' and each of the vertical boundaries mentioned above as an intersection boundary. For any slope section the number of ranges is fixed.

5. The slope surface as well as the layer boundaries are specified by listing the y-coordinates of the points at which they are intersected by the intersection boundaries. Various zones present in the zoned dam are also treated as 'layers'. The geometry of any layer is specified by the co-ordinates of its lower boundary. If in a particular range (segment) a layer (zone) does not exist it has to be treated as the layer of zero thickness in that range or a number of ranges. Layers are numbered from the face of the slope downwards. To illustrate the numbering of the layers, the dam section shown in Fig.2 is chosen, for which the layer numbering is as given in tabular form below the dam section. For example, the layer number 1 which includes the toe weight marked Zone IV has thickness of J_1J_2 and K_1K_2 at the 10^{th} and the 11^{th} intersection boundaries respectively and zero thickness at all other boundaries as at those boundaries it coincides with the slope surface. Similarly, the layer number 2 which includes the shell marked zone III has thickness of G_1G_2, H_1H_2, I_1I_2 and J_2J_3 at the 7^{th}, 8^{th}, 9^{th} and 10^{th} intersection boundaries respectively and zero thickness elsewhere. For the sake of convenience, an axis system different from that in Fig.1 has been chosen for the calculation of slice characteristics.

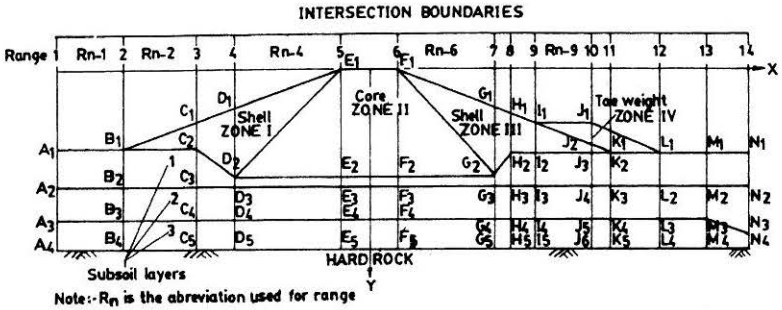

Int. boundary → / Layer number	1	2	3	4	5	6	7	8	9	10	11	12	13	14
Slope surface	A_1	B_1	C_1	D_1	E_1	F_1	G_1	H_1	I_1	J_1	K_1	L_1	M_1	N_1
Layer 1	A_1	B_1	C_1	D_1	E_1	F_1	G_1	H_1	I_1	J_2	K_2	L_1	M_1	N_1
2	A_1	B_1	C_1	D_1	E_1	F_1	G_2	H_2	I_2	J_3	K_2	L_1	M_1	N_1
3	A_1	B_1	C_2	D_2	E_1	F_1	G_2	H_2	I_2	J_3	K_2	L_1	M_1	N_1
4	A_1	B_1	C_2	D_2	E_2	F_2	G_2	H_2	I_2	J_3	K_2	L_1	M_1	N_1
5	A_2	B_2	C_3	D_3	E_3	F_3	G_3	H_3	I_3	J_4	K_3	L_2	M_2	N_2
6	A_3	B_3	C_4	D_4	E_4	F_4	G_4	H_4	I_4	J_5	K_4	L_3	M_3	N_3
7	A_4	B_4	C_5	D_5	E_5	F_5	G_5	H_5	I_5	J_6	K_5	L_4	M_4	N_4

FIGURE 2 : Specification of Layer System in a Typical Heterogeneous Section

From the known values of the co-ordinates of the intersection points of the slope geometry the values of the gradient $\overline{m}$ and the intercept $\overline{c}$ for each of the ranges are calculated using the following expressions:

$$\overline{m} = \overline{m}_{i,j} = \frac{\left(\overline{y}_{i+1,j} - \overline{y}_{i,j}\right)}{\left(\overline{x}_{i+1,j} - \overline{x}_{i,j}\right)} \quad \text{and} \tag{11a}$$

$$\overline{c} = \overline{c}_{i,j} = \frac{\left(\overline{x}_{i+1}\,\overline{y}_{i,j} - \overline{x}_i\,\overline{y}_{i+1,j}\right)}{\left(\overline{x}_{i+1} - \overline{x}_i\right)} \tag{11b}$$

where the equation of the i^{th} range of the j^{th} layer is given by:

$$Y = \overline{m}_{i,j}\,X + \overline{c}_{i,j} \tag{11c}$$

$$i = 1, 2, \ldots, n_R \text{ and}$$

$$j = 1, 2, \ldots, (n_L + 1)$$

where (X, Y) = co-ordinates of any point within the search domain

$\bar{x}_i$ = the x-coordinate of the ith intersection boundary

$\bar{y}_{i,j}$ = the y-coordinate of the ith intersection point of the jth layer

$\bar{m}_{i,j}$ = the gradient of the ith range of the jth layer

$\bar{c}_{i,j}$ = the intercept made by the ith range of the j^{th} layer on the y-axis

n_R = total number of ranges

n_L = total number of layers

In the above, j = 1 refers to the slope surface, j = 2 refers to the layer number 1 and so on.

6. It is required to locate the position of the base of a slice so that appropriate soil and pore pressure properties can be ascribed to it. To do so it is required to locate the two end points of the base. The technique adopted to locate any point (x, y) on the shear surface is explained as follows.

(a) The range i within which the concerned point lies can be found such that

$$\bar{x}_i \leq x \leq \bar{x}_{i+1} \qquad (12a)$$

$$i = 1, 2, \ldots, n_R$$

(b) Similarly, the layer j containing the point can be found such that,

$$y_{dj} \leq y \leq y_{dj+1} \qquad (12b)$$

$$j = 1, 2, \ldots, n_L$$

where, y_{dj+1} is the y-coordinate of the point of intersection of the j^{th} layer boundary with an imaginary vertical line through the given point (x, y) on the shear surface and is calculated as:

$$y_{dj+1} = \bar{m}_{i,j}\, x + \bar{c}_{i,j} \qquad (12c)$$

By repeating (a) and (b) above, the following are found out for a slice:

(i) the range / ranges covering two of its sides.

(ii) the layer / layers containing the two ends of its base.

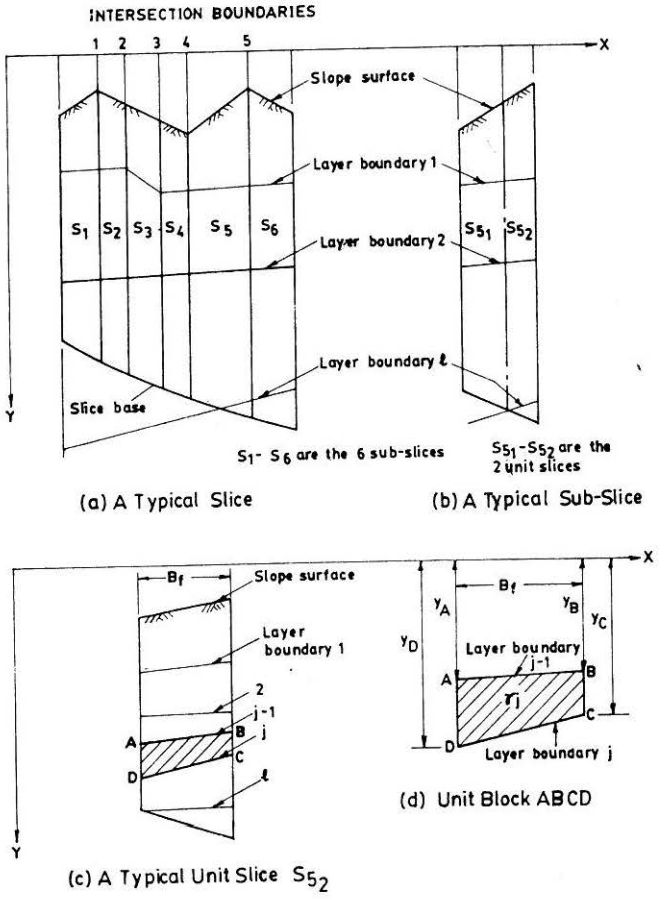

FIGURE 3 : (a) A Typical Slice; (b) A Typical Sub-Slice; (c) A Typical Unit Slice S_{5_2} ; (d) Unit Block ABCD

7. The number of intersection boundaries falling within the width of a slice is noted. If this number is n_B, the entire slice is divided into (n_B+1) number of strips or sub-slices of varying widths. Each of these sub-slices lies entirely within one range. An example of such a slice is shown in Fig.3(a) in which case $n_B = 5$.

8. The y-coordinates of the two ends of the base of a sub-slice can be calculated from the already known values of (i) the y-coordinates of the ends of the base of the original slice, (ii) x-distances of the intersection boundaries and (iii) the inclination of the base of the original slice.

Following step 6, the layers containing the two ends of the base of each of the sub-slices are also found out. Then, taking a sub-slice, it is to

be checked whether its base has been intersected by any layer boundary. If the two bottom ends of the concerned sub slice lie in the same layer, then there is obviously no such intersection. Otherwise, there may be one or more intersections with one or more than one layer boundaries. These are found out by turns. The co-ordinates of such intersection points are calculated by using the known equations of the straight lines representing the base and the particular range of the concerned layer boundary. If the number of such base intersection is n_F, then the number of subdivisions of this sub-slice will be $(n_F + 1)$. These are the most elementary units constituting an original slice; there cannot be any possibility of such a unit being subdivided. Any such unit lies entirely within a range and its base also lies entirely within one layer. Referring to Fig.3(a), it is seen that the sub-slice marked S_5 has been intersected once by a layer boundary, namely, layer 1. So for S_5, the number of elementary units is 2 as shown separately in Fig.3(b).

Weight of a Slice

The weight of an elementary unit described above is the sum total of the weights contributed by each of the layers it has passed through. Referring to Figs.3(c) and 3(d), the weight contributed by the jth layer will be the area of the trapezium ABCD multiplied by the unit weight of that layer.

Let b_F be the width of the unit slice; n_D the deepest layer or the number of layers the unit slice passes through; γ_j the unit weight of the soil of the j^{th} layer and W_{ABCD} the weight of the block ABCD. The weight of the k^{th} elementary slice is then given by:

$$W_{ele_k} = \sum_{j=1}^{n_D} W_{ABCD} \qquad [k = 2 \text{ for } S_{5_2} \text{ in Fig.3(c)}]$$

$$= \sum_{j=1}^{n_D} \frac{1}{2} \gamma_j \, b_F \left\{ (Y_D - Y_A) + (Y_C - Y_B) \right\} \qquad (13a)$$

The weight of one sub-slice (say k^{th}) and, finally, that of an entire slice are given by Eqns.(13b) and (13c) respectively:

$$W_{ss_k} = \sum_{k=1}^{n_F+1} W_{ele_k} \qquad (13b)$$

$$W = \sum_{k=1}^{n_B+1} W_{ss_k} \qquad (13c)$$

Shear Strength Components

Considering that the two ends of a slice-base may lie in different layers, the magnitudes of cohesive and frictional components of shear strength available is likely to vary along a slice-base. However, as the base of an elementary unit described in the previous step lies entirely in a single layer, the cohesive and frictional components calculated for an elementary unit may be summed up to obtain the corresponding values for the entire slice, as follows:

$$\text{Cohesive force component} = \sum_{i=i}^{n_E} c'_i \, \Delta l_i \tag{14a}$$

$$\text{Frictional force component} = \sum_{i=i}^{n_E} \tan\phi'_i \, \Delta l_i \tag{14b}$$

where c'_i and ϕ'_i = shear strength parameters corresponding to the i^{th} elemental unit

Δl_i = length of the base of the i^{th} elemental unit and

n_E = the total number of such elemental units in the entire slice.

If required, the average strength parameters for the slice can be obtained as

$$c'_{av} = \frac{\sum_{i=i}^{n_E} c'_i \, \Delta l_i}{\sum_{i=i}^{n_E} \Delta l_i} \tag{14c}$$

$$\phi'_{av} = \tan^{-1}\left[\frac{\sum_{i=i}^{n_E} \tan\phi'_i \, \Delta l_i}{\sum_{i=i}^{n_E} \Delta l_i}\right] \tag{14d}$$

Pore Water Pressure

The developed computer program for the proposed procedure has the provision for calculation of pore water pressure using two different methods

namely, Method 1 based on the Bishop's pore pressure ratio, r_u and Method 2 based on a given piezometric surface.

Method 1 : This method can be applied to situations where values of r_u are available for all the zones of the dam or embankment section. Following the same principle as discussed in connection with the calculations of cohesive and frictional components of shear strength for an entire slice, the total force, U_b due to pore pressure acting on a slice base may be obtained as follows:

$$U_b = \sum_{i=1}^{n_E} r_{u_i} \sigma_{b_i} \Delta l_i \qquad (15a)$$

where, r_{u_i} is the value of r_u corresponding to the ith unit slice; σ_{b_i} is the average overburden pressure on the base of such a unit. If, for the slice concerned, the average pore pressure on the base is required,, it can be obtained as:

$$u_{av} = \frac{\sum_{i=1}^{n_E} r_{u_i} \sigma_{b_i} \Delta l_i}{\sum_{i=1}^{n_E} \Delta l_i} \qquad (15b)$$

Method 2 : This method is applicable where the piezometric line or surface is available. The pore water pressures are generated using the vertical distances from piezometric surface to the shear surface. In this method, a new set of intersection boundaries are introduced at every point where the given piezometric surface changes directions. These vertical boundaries thus form a number of vertical strips. The distance between any two consecutive boundaries is also referred to as a 'range' with reference to the pore pressure calculation. The original slice may be quite arbitrarily positioned with respect to the vertical strips.

In situations where phreatic line or the top flow line is available in place of the piezometric surface, calculation of pore pressure can be carried out treating the phreatic surface as the piezometric surface. This approximation however, introduces some error. A detailed discussion on this and in general on the methods of pore pressure calculations has been presented by Lambe (1989) and as such they are not stated here. When the phreatic surface is to be used, the first step in using the Method 2 is to approximate the curved surface by a series of straight line segments and then the new set of intersection boundaries are introduced as described above. For example, Figure 4 shows a dam section with an assumed phreatic line which has been

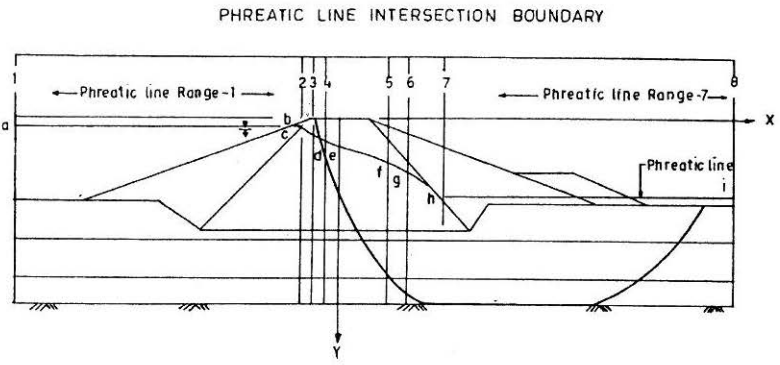

FIGURE 4 : Typical Section of a Zoned Dam along with the Pheratic Line

approximated by 7 linear pieces namely, ab, bc, cd, de, ef, fg, gh and hi. Now, regarding the positioning of the piezometric surface with respect to the base of the various slices, the following four cases may arise:

Case I : Within the strip, the piezometric surface lies entirely above the shear surface [Figure 5(a)]. The force due to pore pressure acting at the base of a single strip or unit is given by:

$$\Delta U_i = \frac{1}{2}\gamma_w (h_L + h_R)\Delta b \sec(\Delta\alpha) \tag{16a}$$

Case II : Within the strip the piezometric surface intersects the base of the strip with its right end going down (Figure 5(b)).

Here the pressure will be caused by only that part of the piezometric surface, which is above the base and is given by:

$$\Delta U_i = \frac{1}{2}\gamma_w h_L x_p \sec(\Delta\alpha) \tag{16b}$$

where, the horizontal distance, x_p, is given by

$$x_p = \frac{(c_2 - c_1)}{(m_1 - m_2)} - x_1 \tag{16c}$$

where, m_1, c_1 and m_2, c_2 are the constants of the following two equations representing the base of the strip and the piezometric line respectively and x_1 is the x-coordinate of the left interslice boundary in Figs.5(b) and 5(c).

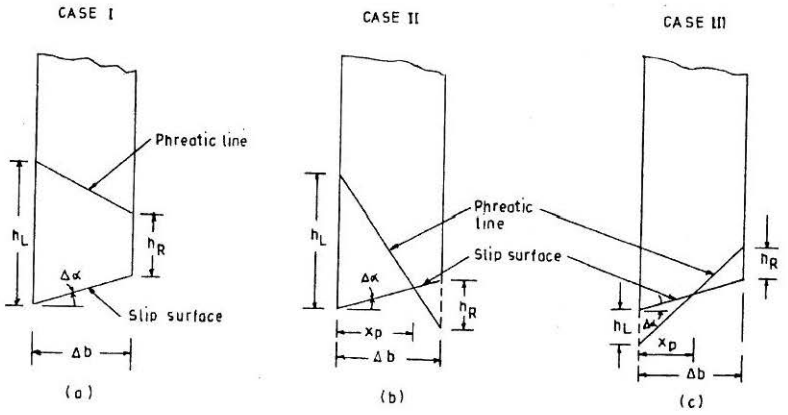

FIGURE 5 : Various Positions of the Pheratic Line with respect to the Slip Surface

$$Y = m_1X + c_1 \text{ and} \tag{16d}$$

$$Y = m_2X + c_2 \tag{16e}$$

Case III : The piezometric surface intersects the base with the left end going down [Figure 5(c)]. Following the same notations as used above,

$$\Delta U_i = \frac{1}{2}\gamma_w h_R(\Delta b - x_p)\sec(\Delta\alpha) \tag{16f}$$

Case IV : The piezometric surface lies entirely below the base of the strip. In this case, for the strip concerned, $\Delta U_i = 0$

Resultant Force Due to Pore Pressure

The resultant force due to pore pressure acting at the base of an original slice is then obtained by adding all the components. If n_p is the number of strip or unit per slice, the resultant force is given by:

$$U_b = \sum_{j=1}^{n_p} \Delta U_i \tag{17}$$

Forces Due to Water Ponding on the Face of the Slope:

The forces exerted by the water ponding on the face of the slope are

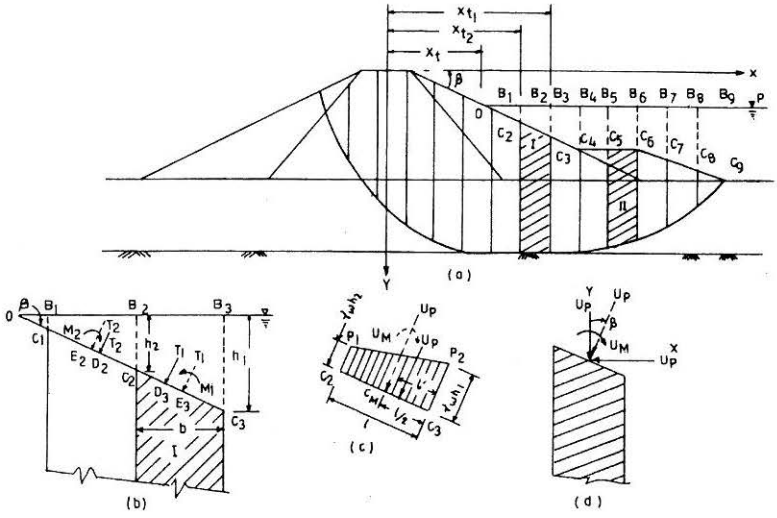

FIGURE 6 : Forces due to Water Ponding on the Face of a Slope

computed slice-wise. Referring to Fig.6(a), it can be seen that two cases may arise and are discussed as follows:

Case I : This case corresponds to slices such as marked 'I' in Fig.6(a). This slice has been separately shown in Fig.6(b). Let h_1 and h_2 be the vertical distances of the two top ends of the slice from the water line measured downward. The trapezoidal pressure diagram has been shown in Fig.6(c). The resultant thrust on the slice U_p acts normally at a distance l' from C_3 where,:

$$U_p = \text{Area of the trapezium } P_1C_2P_2C_3$$

$$= \frac{1}{2}\gamma_w(h_1 + h_2)l \tag{18a}$$

where, $$l = \sqrt{b^2 + (h_1 - h_2)^2} \tag{18b}$$

and, $$l' = \frac{1}{3}\left[\frac{h_1 + 2h_2}{h_1 + h_2}\right] \tag{18c}$$

This is equivalent to a force U_p acting at the mid-point C_M together with a couple in the clockwise sense of moment

$$U_M = U_p\left(\frac{1}{2} - l'\right) \tag{19a}$$

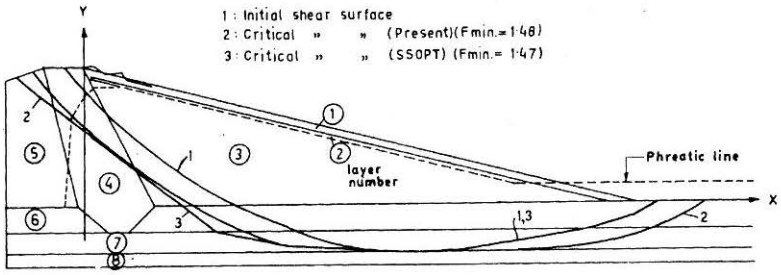

Layer No.	1	2	3	4	5	6	7	8
c' (kPa)	0.00	0.00	0.00	10.00	0.00	30.00	10.00	2000
ϕ' (deg.)	42.00	30.00	30.00	19.00	30.00	30.00	19.00	20.00
γ (kN/m^3)	18.50	18.50	19.80	18.80	18.00	18.50	19.50	20.00

FIGURE 7 : Critical Shear Surfaces for the Example Problem

Case II : This case corresponds to slices marked II in Fig.6(a) which are bounded by the horizontal surface. For this case $h_1 = h_2$ and, hence, $l = b$ and $l' = 1/2$, which make, $U_M = 0$.

For the sake of convenience in including these forces in the formulation, U_p has been resolved horizontally and vertically, as shown in Fig.6(d), giving:

$$U_p^X = U_p \sin\beta \tag{19b}$$

$$U_p^Y = U_p \cos\beta \tag{19c}$$

The Program SUMSTAB

The scope of the program SUMSTAB originally developed and reported for homogeneous slopes (Bhattacharya and Basudhar, 2000b), has been extended to nonhomogeneous slopes such as slopes of zoned dams and embankments founded on layered deposits having any arbitrary variation of soil and pore pressure conditions. It should be mentioned, however, that in its present form, the program is capable of analysing a dam section only for the steady seepage condition.

Illustrative Example: The Okete Dam Upstream Slope

Figure 7 shows a section of the Okete dam upstream slope along with the layering, soil properties and the phreatic line. The ordinates of the various points on the dam section including the layer boundaries and the phreatic line have been taken from a manual by Baker (1979) who has presented detailed

results of analysis of the same section with the help of the program SSOPT which is based on the dynamic programming technique in conjunction with the Spencer's method (1967). In the said analysis, pore pressures have been generated using vertical distances below the phreatic line shown in the Figure. This phreatic line is reportedly a top flow line and the forces due to water ponding on the face of the slope have been considered in the analysis. The purpose of selecting this case study as the illustrative example in the present study is the following:

(i) to test the effectiveness and efficiency of the proposed numerical scheme in handling a zoned dam with a complex geometry, layering and a steep phreatic line.

(ii) to draw a comparison between the results obtained by using the program SSOPT based on the dynamic programming technique and the developed program SUMSTAB based on the sequential unconstrained minimization technique.

Results and Discussion

Previous Solution by Baker using the Program SSOPT

As already stated, the problem was solved earlier by Baker (1979) using the program SSOPT. The critical shear surface given by the program SSOPT based on the dynamic programming technique coupled with the Spencer's method, as reported by Baker (1979) is also presented in Fig.7. The values of F_{min} and θ were reported to be 1.467 and 8.976 degrees respectively. The calculated values of various slice characteristics associated with the critical surface were also reported in the form of a computer output of the program SSOPT, which is not reproduced here to save space. It is, however, seen from the said output (Baker, 1979) that the resultant interslice forces as well as the normal forces at the slice bases are all positive, as they should be. The positions of the line of thrust for total stress are also reasonable. However, the line of thrust for effective stress has not been reported.

Present Solution

Before proceeding with the critical surface determination, the critical surface reported by Baker has been re-analysed using the program SOLVE developed by the authors (Bhattacharya and Basudhar, 2000b) and the obtained values ($F = 1.466$, $\theta = 8.976°$) are observed to be in perfect agreement with those reported by Baker. The slice configurations used in Baker's analysis have also been used in the present re-analysis of Baker's critical surface.

The critical slip surface obtained in the present analysis is also presented in Fig.7. A total of 19 slices has been used in the computation. The initial trial slip surface is also shown in the Figure. The corresponding F_{min} and θ have been obtained as 1.48 and 8.706 degrees respectively which are quite close to the value of 1.47 (rounding off to two decimal places) and 8.976 corresponding to the critical surface reported by Baker. However, as seen from the figure, the two critical surfaces are quite different from each other especially towards the toe, the present critical surface being much deeper.

The calculated responses associated with the obtained critical surface are presented in Table 1. The positions of the line of thrust for total stress and that for effective stress are indicated by the ratios L/H and L′/H respectively, where, L and L′ denote heights of the points of application of the total and effective interslice forces respectively and H is the height of the corresponding interslice boundary. Z, Z′, σ, σ' and τ denote the resultant interslice force, normal component of the effective interslice force, the total normal stress, the effective normal stress and shear stress at the base of a slice respectively. For the expressions for each of the above, reference may be made to Spencer (1973) and Bhattacharya (1990). It can be seen from the Table that the line of thrust for total stress as well as for effective stress lie within the middle third except at a couple of interslice boundaries near the upper end. The effective interslice forces (Z') as well as the effective normal stress (σ') and shear stresses (τ) at the slice bases are all positive and hence the line of thrust can be accepted as reasonable. It may be mentioned, however, that the determination of the position of the line of thrust for effective stress as also the pore water pressure is based on treating the phreatic line as the piezometric line and, hence, is approximate. Attempt to find a more acceptable line of thrust by introducing tension crack and treating the same as a design variable, has been demonstrated elsewhere for the case of homogeneous slopes (Bhattacharya and Basudhar, 2000b). Such an attempt has not been made in this case in view of the difficulty in estimating the depth of tension crack in a layered soil. Alternatively, analyses may be carried out taking arbitrary depths for tension crack and keeping it constant during the search; however, no such attempt has been made here in view of the satisfactory values of the internal forces.

Table 2 presents the values of the design vector and the design constraints at the starting point and at the optimal point corresponding to the solution presented above. The Table indicates that even though the initial design vector is infeasible with regard to both equality and inequality constraints (the violated constraints are marked as underlined), the proposed scheme utilizing the Extended Interior Penalty

Table 1 : Calculated Responses Associated with the Critical Slip Obtained in the Present Analysis

Slice No.	σ kPa	σ' kPa	τ kPa	L/H	L'/H	Z kN/m	Z' kN/m
1	111.6	70.7	36.0				
				0.56	0.40	500.0	253.2
2	164.9	101.3	41.1				
				0.48	0.47	1109.0	754.2
3	187.3	110.9	26.2				
				0.45	0.47	1446.0	966.8
4	217.2	127.5	31.8				
				0.42	0.44	1784.0	1257.0
5	240.5	141.5	35.7				
				0.41	0.44	2094.0	1564.0
6	264.1	163.3	39.4				
				0.41	0.45	2388.0	1804.0
7	285.5	182.0	43.1				
				0.39	0.44	2625.0	1837.0
8	310.1	195.8	46.9				
				0.38	0.43	2864.0	1929.0
9	335.9	206.3	48.2				
				0.37	0.42	3069.0	1971.0
10	350.7	209.0	48.1				
				0.36	0.43	3213.0	1692.0
11	361.2	216.4	48.5				
				0.35	0.39	3235.0	1634.0
12	366.3	188.0	48.0				
				0.35	0.40	3150.0	1512.0
13	320.8	146.6	62.3				
				0.34	0.38	2616.0	1178.0
14	287.4	128.1	67.7				
				0.31	0.31	2118.0	968.2
15	262.4	121.0	47.2				
				0.30	0.28	1583.0	693.8
16	227.9	103.9	40.5				
				0.26	0.23	1026.0	362.9
17	182.5	91.4	33.3				
				0.25	0.21	481.8	250.2
18	118.3	65.4	26.1				
				0.31	0.31	97.3	96.2
19	39.7	39.7	15.5				

Function method brings out an optimal solution which is entirely in the feasible region. Thus it is seen that, the proposed Direct Procedure is capable of handling the equality constraint as well as infeasible initial design vector quite efficiently. Similar observation has been made elsewhere with respect to homogeneous slopes (Bhattacharya and Basudhar, 2000b).

Table 2 : Design Vector and Constraints for the Example Problem

STARTING POINT

δ_1	ε_o	f	ψ	F	θ	Z_n	M_n
0.001	−0.1	1.25	1.3448	1.25	0.1000	0.1033×10^3	0.2332×10^4

Design Variables : 22 Variables for 19 Slices

−2.6667	−4.4444	−5.7778	−6.4444	−6.9778	−6.9999	−6.9999	−6.9999
−6.9999	−5.9999	−5.1111	−3.7778	−1.9999	0.0000	2.6889	6.1111
10.5778	15.3778	96.0000	−3.0000	1.2500	0.1000		

Constraints (inequality) :

−0.9398	−0.7884	−0.7695	−0.7520	−0.7256	−0.6928	−0.6623	−0.6296
−0.5936	−0.5616	−0.5150	−0.4779	−0.4453	−0.3997	−0.3287	−0.2519
−0.1747	−0.1127	−0.8890	−0.4443	−0.6668	−0.1332	−0.5113	−0.0221
−0.0000	0.0000	0.0000	0.1112	−0.4445	−0.4446	−0.2220	−0.6890
−0.7333	−1.0445	−0.3333	−0.8222	−0.5980	−0.5843	−0.5366	−0.4588
−0.4172	−0.3831	−0.3629	−0.3413	−0.3172	−0.2849	−0.2561	−0.2162
−0.1481	−0.0624	0.0898	0.4220	1.3823	3.6408	−0.4020	−0.4157
−0.4633	−0.5312	−0.5828	−0.6169	−0.6370	−0.6587	−0.6828	−0.7150
−0.7439	−0.7838	−0.8519	−0.9376	−1.0898	−1.4219	−2.3823	−4.6407
−0.2600	−0.1000						

Constraint (equality) : 0.3456E+00

Table 2 : Continued

OPTIMAL POINT

δ_t	ε_o	f	ψ	F	θ	Z_n	M_n
0.001	-1.0×10^{-8}	1.4835	1.4855	1.4835	0.1519	0.2933×10^{-2}	-0.1843×10^{-1}
Design Variables : 22 Variables for 19 Slices							
−2.5382	−4.5821	−5.3997	−6.1077	−6.6261	−6.9409	−6.9999	−6.9990
−6.9394	−6.5540	−5.9199	−5.0073	−2.3489	0.5702	3.5059	6.8329
10.7466	15.0999	87.8154	−10.3439	1.4835	0.1519		
Constraints (inequality) :							
−1.0000	−1.0000	−0.8635	−0.8089	−0.7766	−0.7463	−0.7196	−0.6753
−0.6323	−0.5865	−0.5359	−0.4897	−0.4527	−0.4022	−0.3260	−0.2391
−0.1665	−0.0908	−0.0014	−0.9768	−0.3347	−0.2952	−0.1567	−0.2547
−0.0776	−0.0027	−0.3605	−0.3432	−0.0922	−2.0383	−0.0119	−0.0037
−0.0223	−0.7552	−1.1883	−0.0012	−0.6989	−0.6462	−0.6100	−0.5317
−0.4780	−0.4539	−0.4414	−0.4206	−0.3992	−0.3838	−0.3735	−0.3653
−0.3533	−0.3263	−0.3098	−0.2868	−0.2442	−0.3186	−0.3011	−0.3538
−0.3899	−0.4683	−0.5220	−0.5461	−0.5586	−0.5794	−0.6008	−0.6162
−0.6265	−0.6347	−0.6467	−0.6737	−0.6902	−0.7132	−0.7558	−0.6814
−0.4935	−0.1519						

Constraint (equality) : 0.1268E−09
No. of r−minimization required = 7

Note : Out of a total of 22 design variables, the first 18 denote the y-coordinates and the next two denote the x-coordinates of the two ends of a potential shear surface while the last two are the variables F and θ. Out of a total of 74 inequality constraints, First 18 are boundary constraints, next 18 are curvature constraints, next 36 are constraints on line of thrust and the last two are side constraints on F and θ respectively

Table 3 : Progress of Minimization in the Example Problem

No. of r−minimization	Value of r	Objective function f	Composite function ψ	Z_n kN/m	M_n kN−m/m
0 (Starting Point)	1×10^{-4}	1.2500	1.3448	0.1033×10^{3}	0.2332×10^{4}
1	1×10^{-4}	1.0002	1.0475	0.3238×10^{3}	-0.3431×10^{3}
2	1×10^{-5}	1.0019	1.1753	0.2874×10^{3}	0.4814×10^{3}
3	1×10^{-6}	1.3943	1.4553	0.5303×10^{2}	-0.7395×10^{1}
4	1×10^{-7}	1.4786	1.4928	0.1499×10^{2}	-0.1055×10^{2}
5	1×10^{-8}	1.4818	1.4894	0.2181×10^{1}	0.2142×10^{2}
6	1×10^{-9}	1.4835	1.4856	0.5933×10^{-1}	0.2737×10^{0}
7 (Optimal Point)	1×10^{-10}	1.4835	1.4855	0.2933×10^{-2}	-0.1842×10^{-1}

Progress of Minimization

The progress of the minimization can be studied from Table 3 which presents the variation of the function values f and ψ with the number of r-minimizations. It is seen that initially the function values go on decreasing to reach some lowest values and then show a tendency to increase till they converge to the feasible minimum. On inspection of the detailed results it has been observed that in the first few cycles the function values decrease continually during which the numerical scheme shows a tendency to keep all the inequality constraints satisfied. However, at these stages the equality constraint remains violated i.e., its value does not diminish sufficiently. Afterwards, the minimization procedure attempts to effectively satisfy the equality constraint by re-adjusting two design variables in particular, namely, F and θ. This eventually results in subsequent increase in the values of the functions f and ψ till finally the convergence is achieved. The trend observed here is the same as has been observed in the case of homogeneous slopes (Bhattacharya and Basudhar, 2000b).

Conclusions

Based on the studies reported in this paper, the following conclusions are drawn:

1. The proposed methodology based on the Spencer method of analysis coupled with the sequential unconstrained minimization technique of nonlinear programming promises to be an effective and efficient tool

for determining the critical slip surface and the associated minimum factor of safety of nonhomogeneous slopes.

2. The program SUMSTAB developed as a FORTRAN version of the proposed Direct procedure can handle any complex geometry of a zoned dam section founded on a stratified deposit with any number of arbitrarily aligned layers having various soil and pore pressure characteristics under steady seepage condition

3. For the case study reported herein, the results obtained using the program SUMSTAB based on the developed procedure are comparable to that yielded by the program SSOPT also based on Spencer method of analysis but coupled with a different minimization procedure namely, the dynamic programming technique which is known to yield global minimum. It is observed that the value of the minimum factor of safety obtained by using the two programs are in close agreement with each other; the corresponding critical slip surfaces, are, however, markedly different.

4. From the observation stated above it appears that it is the shape and location of the critical shear surface rather than the value of the minimum factor of safety, which is more sensitive to the methodology used for their determination. The closeness of the factor of safety of the two shear surfaces (evaluated by the same method of analysis, e.g., the Spencer method) wide apart from each other also indicates the presence of a critical zone rather than a sharply defined critical slip surface.

References

BAKER, R. (1979) : "SSOPT :- A Computer Program for Determination of the Critical Slip Surface in Slope Stability Computations - Users' Manual", *Faculty Publication No. 253*, Israel Institute of Technology, Haifa, Israel.

BAKER, R. (1980) : "Determination of the Critical Slip Surface in Slope Stability Computations", *International Journal for Numerical and Analytical Methods in Geomechanics*, 4 , 333-359.

BASUDHAR, P.K, YUDHBIR and BABU, N.S. (1988) : "SUMSTAB - A Computer Software for Generalised Stability Analysis of Zoned Dams", *Proc. of the Sixth Int. Conf. on Numerical Methods in Geomechanics*, Innsbruck, 1407-1412.

BHATTACHARYA, G. (1990) : "Sequential Unconstrained Minimization Technique in Slope Stability Analysis", *Ph. D. Thesis*, Indian Institute of Technology, Kanpur, India.

BHATTACHARYA, G. and BASUDHAR, P.K. (1992) : "Some Factors Involved in Solving the Stability Equations of General Slip Surfaces", *Proc. Indian Geotechnical Conference*, Calcutta, 453-456.

BHATTACHARYA, G. and BASUDHAR, P.K. (1999) : "A New Approach of Solving the Stability Equations of General Slip Surfaces", *Indian Geotechnical Journal*, Vol.29, No.4, 322-338.

BHATTACHARYA, G. and BASUDHAR, P.K. (2000a) : "Slope Stability Computations in Nonhomogeneous and Anisotropic Soils", *Indian Geotechnical Journal*, Vol.30, No. 4, pp.385- 399.

BHATTACHARYA, G. and BASUDHAR, P.K. (2000b) : "A New Procedure for Finding Critical Slip Surfaces in Slope Stability Analysis", Accepted for publication in the Indian Geotechnical Journal.

CASSIS, J.H. and SCHMIT, L.A. Jr. (1976) : "On Implementation of the Extended Interior Penalty Function", *International Journal for Numerical Methods in Engineering*, Vol.10, 3-23.

CELESTINO, T.B. and DUNCAN, J.M. (1981) : "Simplified Search for Noncircular Slip Surfaces", *Proc. of Tenth Int. Conf. on Soil Mechanics and Foundation Engineering*, Stockholm, 3, 391-394

FOX, R.L. (1971) : *Optimization Methods for Engineering Design*, Addison-Wesley, Reading, Mass.

GRECO, V.R. (1988) : "Numerical Methods for Locating the Critical Slip Surface in Slope Stability Analysis", *Proc. of the Sixth Int. Conf. on Numerical methods in Geomechanics*, Innsbruck, 1219-1223.

JANBU, N. (1973) : "Slope Stability Computations", *Embankment Dam Engineering, Casagrande Volume*, Edited by R.C. Hirschfeld and S.J. Poulos, John Wiley & Sons, New York, 47-86.

KAVLIE, D. (1971). "Optimum Design of Statically Indeterminate Structures", *Ph.D. Thesis*, University of California at Berkeley, CA.

KAVLIE, D. and MOE, J. (1971) : "Automated Design of Frame Structures", *Journal of Structural Division*, ASCE, Vol.97, No.ST1, 33-62.

LAMBE, T.W. (1989) : "Expressing the Level of Stability of a Slope", *The Art and Science of Geotechnical Engineering At the Dawn of the Twenty First Century* – A Volume honouring R.B. Peck, Edited by E.J. Cording, W.J. Hall, J.D. Halliwanger, A.J. Hendrin Jr., G. Mesri, Prentice Hall.

NGUYEN, V.U. (1985) : "Determination of Critical Slope Failure Surfaces", *Journal of the Geotechnical Engrg.* Div., ASCE, Vol.111, 238-250.

SATYAM BABU, N. (1986) : "Optimization Techniques in Stability Analysis of Zoned Dams", *M. Tech Thesis*, Indian Institute of Technology, Kanpur.

SPENCER, E. (1967) : "A Method of Analysis of the Stability of Embankments Assuming Parallel Interslice Forces", *Geotechnique*, 17, No.1, 11-26.

SPENCER, E. (1973) : "The Thrust Line Criterion in Embankment Stability Analysis", *Geotechnique*, 23, 85-101.